# Direct Measurement of Methane Hydrate Composition along the Hydrate Equilibrium Boundary

**Susan Circone, Stephen H. Kirby, and Laura A. Stern***

*United States Geological Survey, 345 Middlefield Road MS 977, Menlo Park, California 94025*

*Received: January 27, 2005; In Final Form: March 18, 2005*

The composition of methane hydrate, namely $n_w$ for $CH_4 \cdot n_w H_2O$, was directly measured along the hydrate equilibrium boundary under conditions of excess methane gas. Pressure and temperature conditions ranged from 1.9 to 9.7 MPa and 263 to 285 K. Within experimental error, there is no change in hydrate composition with increasing pressure along the equilibrium boundary, but $n_w$ may show a slight systematic decrease away from this boundary. A hydrate stoichiometry of $n_w = 5.81-6.10$ $H_2O$ describes the entire range of measured values, with an average composition of $CH_4 \cdot 5.99(\pm 0.07)H_2O$ along the equilibrium boundary. These results, consistent with previously measured values, are discussed with respect to the widely ranging values obtained by thermodynamic analysis. The relatively constant composition of methane hydrate over the geologically relevant pressure and temperature range investigated suggests that in situ methane hydrate compositions may be estimated with some confidence.

## Introduction

Structure I methane hydrate is a crystalline compound comprised of a hydrogen-bonded $H_2O$ lattice with small (pentagonal dodecahedral) and large (tetrakaidecahedral) cages that may each contain a molecule of $CH_4$ gas. The structure I unit cell consists of 46 $H_2O$ molecules and eight such cages, in a ratio of one small to three large. If all cages are filled with methane, then the composition is $CH_4 \cdot 5.75H_2O$, where 5.75 is referred to as the hydrate number $n_w$. However, it is well-known that, unlike the salt hydrate compounds, gas clathrate hydrates are nonstoichiometric with some cages vacant (i.e., $n_w$ is greater than 5.75 for structure I hydrates). Historically, measurement of gas hydrate composition has been difficult (see discussion in Sloan[1]), primarily due to the presence of free $H_2O$ in addition to that in the hydrate structure. Laboratory-made hydrates typically contain unreacted, occluded free $H_2O$ that cannot easily be removed or independently measured. Additional difficulties arise in measuring the compositions of naturally occurring hydrates, which typically coexist with free $H_2O$ and also undergo partial dissociation during recovery. Thus, measurement of hydrate composition has yielded a wide range of values for $n_w$ for many gas hydrates, including methane.

Several techniques have been used previously to measure the composition of $CH_4$ hydrate samples. A common technique involves thermodynamic analysis of the pressure, temperature ($P$,$T$) slopes of the hydrate dissociation reactions

$$CH_4 \cdot n_w H_2O(s) = CH_4(g) + n_w H_2O(s) \quad (1)$$

and

$$CH_4 \cdot n_w H_2O(s) = CH_4(g) + n_w H_2O(l) \quad (2)$$

at the quadruple point $Q$, the intersection between the hydrate stability boundary and the $H_2O$ solid/liquid boundary (Figure 1). Through the use of the Clapeyron equation

$$\frac{dP}{dT} = \frac{\Delta H}{T\Delta V} \quad (3)$$

the enthalpy of each reaction can be calculated. Hydrate

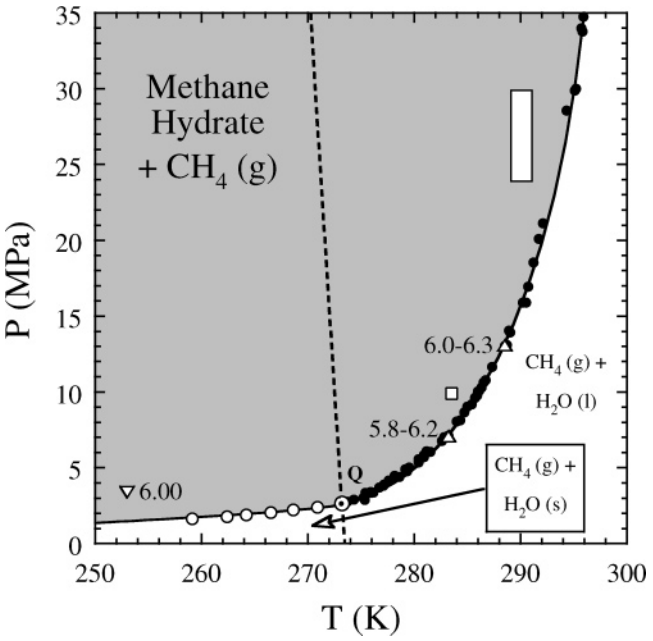


**Figure 1.** Phase diagram for the $CH_4-H_2O$ system, where methane hydrate coexists with excess $CH_4$(g). The phase equilibria data for reaction 1 (○) and reaction 2 (●)[1] as well as the stability boundary for methane hydrate (−) and the solid/liquid boundary for $H_2O$ (- - -) are shown. The intersection of these two boundaries defines the quadruple point $Q$, where hydrate + gas + ice + water coexist. In the presence of excess $CH_4$, the $H_2O$ solid/liquid boundary is metastable in the hydrate stability field. Also plotted are the $P$,$T$ synthesis conditions of methane hydrate samples and published measurements of hydrate numbers from Galloway et al.[6] (△) and Handa[8] (▽). In addition, the final $P$,$T$ synthesis conditions for our samples are also indicated (□).

* Author to whom correspondence should be addressed. Phone: (650) 329-4811. Fax: (650) 329-5163. E-mail: lstern@usgs.gov.

10.1021/jp0504874 CCC: $30.25 
Published on Web 04/22/2005

stoichiometry is then calculated using the relationship

$$n_w = \frac{\Delta H_2 - \Delta H_1}{\Delta H_{m,H_2O}} \quad (4)$$

where $\Delta H_{m,H_2O}$ is the enthalpy of melting of $H_2O$ at the quadruple point in joules per mole. In other words, the difference in slope and therefore enthalpy between reactions 1 and 2 is assumed to be equivalent to the enthalpy needed to melt $n_w$ moles of $H_2O$. Reaction enthalpies are assumed to be constant over the *P*,*T* range of the analysis. Through the use of this technique, values for $n_w$ between 5.77 and 7.4 have been reported for methane hydrate.[2−6]

Methane hydrate stoichiometry has also been determined by direct measurement,[6] calculated from the mass decrease in free gas in a system following conversion of liquid water to hydrate and from the amount of gas released by dissociating the hydrate at constant pressure. Calculated values include corrections for dissolved gas in water and increasing temperature to promote dissociation. Experimental hydrate numbers range between 5.84 and 6.16 at 283.2 K and 7.1 MPa and between 6.01 and 6.34 near 288.5 K and 13.1 MPa. These measured compositions do not show the expected decrease in hydrate number with increasing synthesis pressure, as predicted from the theoretical model based on statistical thermodynamics. This expected trend has been demonstrated for other structure I hydrates ($H_2S$, $SO_2$, Xe, $Cl_2$, $CH_3Cl$, $CH_3Br$, and $CHClF_2$) by direct measurement.[7]

A hydrate composition of $CH_4 \cdot 6.00H_2O$ was determined using calorimetry on a sample synthesized at 253 K and 3.4 MPa (final conditions).[8] Specifically, the hydrate number was measured directly from the ratio of the amount of water in the hydrate to the amount of gas released by dissociation via reaction 1. This technique has several advantages, most importantly providing a means of directly measuring the amount of free $H_2O$ in the sample prior to dissociation (from a measured enthalpy change as *P*,*T* conditions cross the $H_2O$ ice/liquid boundary. No free water was detected in the methane hydrate sample). In addition, Handa[9] confirmed that the difference in enthalpy for reactions 1 and 2 is equivalent, within experimental error, to $n_w$ times $\Delta H_{m,H_2O}$ (6009 J/mol at 273.15 K and 0.1 MPa).

Recently, methane hydrate composition has been inferred using Raman spectroscopy.[10] Relative cage occupancies are determined from their respective peak areas, after subtracting the contributions of excess water and free methane gas to the spectra. If one assumes that all large cages are completely filled, then hydrate numbers of 5.81 to 5.96 (±0.05) are obtained for hydrate grown at 275.15 K and 30 MPa in the presence of excess methane gas or excess water, respectively. If vacancies are present in the large cages, then $n_w$ is shifted to higher values.

To summarize, a few direct measurements of methane hydrate stoichiometry have been made, yielding compositions near $CH_4 \cdot 6H_2O$. These results do not indicate a decrease in hydrate number with increasing pressure from 3.4 to 13.1 MPa (Figure 1). Thermodynamic analysis of the dissociation curves yield widely varying results for $n_w$ (5.77 to 7.4). Prediction of in situ methane hydrate compositions remains an important issue to resolve, so that (1) the extent of dissociation and sample alteration during drill core recovery can be ascertained and (2) accurate gas production models can be developed.

We have undertaken a systematic measurement of the hydrate number along the equilibrium boundary at conditions primarily above the quadruple point. We start with methane hydrate samples synthesized in the presence of excess methane gas at pressures well above the equilibrium boundary. The absence of unreacted water following synthesis is determined for each sample (see below). After annealing the sample at various conditions along the equilibrium boundary, we then directly measure the amount of gas in the sample by dissociating the hydrate under constant pressure conditions. We present results on how the hydrate number changes along the equilibrium curve and how $n_w$ changes if hydrate annealing conditions are at elevated pressures above the equilibrium boundary. We also discuss the calculation of hydrate number by analysis of the Clapeyron slopes of the dissociation curves.

## Experimental Methods

Methane hydrate samples were synthesized in a pressure vessel, using the method and apparatus described by Stern et al.,[11,12] from nominally 26 g of granulated $H_2O$ ice (180−250 $\mu$m grain size) and pressurized $CH_4$ gas. Hydrate formation occurred as the reactants were heated from 250 to 290 K while $CH_4$ pressure increased from 22 ± 2 to 27 ± 3 MPa due to heating at an approximately constant volume ($P_{equil}$ is 16 MPa at 290 K). The reaction went to completion after 30−48 h at 290 K, as pressure slowly decreased then stabilized. Complete reaction of all $H_2O$ to hydrate was confirmed by the absence of abrupt increases in pressure and temperature as samples were cooled through the $H_2O$ solid−liquid boundary. If a freezing signal was detected, then the heating cycle was repeated until no freezing anomaly was observed. The measured composition of $CH_4$ hydrate synthesized near these conditions is $CH_4 \cdot 5.89 H_2O$, with an accuracy of ±0.06 (±1 mol % of $CH_4$ gas).[13] Two additional samples, 011604A and B, were synthesized with final conditions at 283.5 K and 9.9 MPa (pressure varied between 9.4 and 9.9 MPa during synthesis; $P_{equil}$ is 7.6 MPa at 283.5 K).

After the synthesis, samples were cooled to 253 K under high methane pressure. The sample pressure vessels were transferred under pressure to a precision Hart standard bath (model 7081-CSI) at 253 K. (Note that the use of trade, product, industry, or firm names in this report is for descriptive purposes only and does not constitute endorsement by the U. S. Government.) Temperature was then raised to the selected temperature for the experiment. The d-limonene bath surrounding the pressure vessel was maintained at constant temperatures to within ±0.002 K, and the bath temperature was measured independently to within ±0.006 K using a calibrated Hart platinum resistance thermometer (PRT, model 5627-12, attached to a Hart 1502A electronic box). The internal temperature of the hydrate sample was monitored during the experiments with chromel−alumel (type K) thermocouples, referenced to a Hart Scientific zero point calibrator (model 9101). Internal sample temperature was monitored using one of two configurations, (1) three thermocouples along the cylindrical axis of the sample (top, middle, and bottom) and one at the middle of the sample side or (2) one centered thermocouple. Thermocouples were calibrated to the high-precision bath PRT in every experiment under conditions of constant *T* within the hydrate stability field and were accurate to ±0.05 K.

After a sample had thermally equilibrated with the high-precision bath, methane pressure was lowered to conditions just above the equilibrium boundary by venting gas from the vessel. The sample was then opened to a back-pressure regulator (Tescom model ER 3000) set at the selected pressure. The back-pressure regulator, located between the sample and a custom flowmeter,[13] has a maximum working pressure of 10 MPa. Pressure was monitored continuously with a pressure transducer

**TABLE 1: Methods and Final *P*,*T* Conditions for Annealing Methane Hydrate Samples Prior to Dissociation**

| experiment ID[a] | anneal method[b] | $T$ (K) | $P_{equil}$[c] (MPa) | $P_{initial}$ (MPa) | $P_{ice}$[d] (MPa) | $P_{final}$ (MPa) | time at $P_{final}$ (h) | total anneal time (h) |
|---|---|---|---|---|---|---|---|---|
| 050203B | Ia | 263.09 | 1.9 | 2.00 | | 1.88 | 670.5 | 788 |
| 051304A | Ia | 268.15 | 2.1 | 2.29 | | 2.29 | | 329 |
| 082003B | Ia | 273.15 | 2.6 | 2.74 | | 2.74 | | 239 |
| 100903A | II | 275.15 | 3.2 | 3.28 | 3.28 | 3.47 | 45.7 | 62 |
| 051304B | Ib | 275.15 | 3.2 | 3.29 | | 3.28 | | 143 |
| 110403B | II | 277.15 | 3.9 | 4.13 | 3.93 | 4.05 | 41.5 | 232 |
| 120303B | II | 279.15 | 4.8 | 4.91 | 4.72 | 4.81[e] | 70.1 | 501 |
| 120303A | III | 279.15 | 4.8 | 9.62 | | 9.61 | 94.6 | 95 |
| 100903B | II | 281.15 | 5.9 | 6.07 | 5.90 | 6.00 | 24.8 | 216 |
| 090903B | II | 283.15 | 7.3 | 7.42 | 7.42 | 7.50 | 24.5 | 264 |
| 011604A | V | 283.50 | 7.6 | | | 9.90 | | |
| 011604B | IV | 284.15 | 8.1 | | | 9.68 | | 21 |
| 042204B | Ib | 285.15 | 9.0 | 9.52 | | 9.07 | 43.0 | 145 |
| 090903A | II | 285.15 | 9.0 | 9.13 | 9.13 | 9.62[e] | 24.2 | 263 |

[a] Experiment ID indicates original date of synthesis. A or B indicates whether the pressure vessel contained one or four thermocouples, respectively. [b] Annealing methods are defined in the Experimental Methods section. Method III further involved a heating cycle from 279.15 to 283.15 K, with conditions remaining within the hydrate stability field. An additional 0.0007 mol of methane were released after reaching the higher *T*. The total anneal time includes this thermal cycle. [c] $P_{equil}$ values were extrapolated from the published phase equilibria data[1] (Figure 1). [d] $P_{ice}$ is the annealing pressure after which a freezing anomaly was observed during thermal cycling. [e] The cooling cycle still contained a barely detectable freezing anomaly ($\ll$1 K).

calibrated to a digital Heise gauge (model ST-2H). The back-pressure regulator maintained pressure on the sample to within $\pm$0.03 MPa of the set point by releasing gas to the flowmeter (see below). Gas release from the sample was monitored using the flowmeter, in which released gas is collected at 0.1 MPa. The gas flow rate is determined by monitoring the change in weight of an inverted, $H_2O$-filled, close-ended cylinder as released gas displaces the $H_2O$.[13]

Prior to dissociation, most samples were equilibrated at conditions near the methane hydrate equilibrium boundary using one of two methods (Table 1). In method I, samples were annealed at constant *P*,*T* conditions just within the hydrate stability field until gas evolution from the sample stopped. The back-pressure regulator maintained isobaric conditions by releasing the gas to the flowmeter. Samples annealed at temperatures $\leq$273 K were not thermally cycled through the ice melting point to recheck for the presence of free $H_2O$ (method Ia). For annealing conditions above 273 K, the sample was thermally cycled, and no freezing signals were detected (method Ib).

In method II, the hydrate was partially dissociated then regrown to promote sample equilibration at near-equilibrium conditions prior to the determination of $n_w$. Again, samples were first annealed at constant *P*,*T* conditions until gas evolution from the sample stopped. Samples were then thermally cycled (Figure 2). If no freezing anomaly was detected, the pressure was decreased (usually by 0.1 MPa), and the sample was annealed at least 15 h before repeating the thermal cycling. This sequence of steps was repeated until the appearance of a freezing signal indicated that a small amount of dissociation had occurred (i.e., free $H_2O$ was now present). Then, the process was reversed by incrementally increasing the pressure until the freezing anomaly was no longer detectable. During this portion of the anneal, pressure on the sample was controlled manually rather than by the back-pressure regulator, and no gas release to the flowmeter occurred.

After the sample was annealed, the vessel was again opened to the back-pressure regulator−flowmeter system. Samples were dissociated by increasing the surrounding bath temperature such that final *P*,*T* conditions on the sample were outside the methane hydrate stability field. As sample conditions reached the equilibrium boundary, dissociation began and then proceeded to completion, while the back-pressure regulator maintained a constant pressure and the released gas collected in the flowmeter at 0.1 MPa (Figure 3). During dissociation, the hydrate temperature stalled at either the hydrate stability boundary (Figure 3, for *P* above the quadruple point) or the $H_2O$ solid/liquid boundary (at *P* below the quadruple point, not shown). The latter behavior has been described and discussed in detail previously.[14−16]

In addition, one sample was annealed at 279.15 K and 9.6 MPa, twice $P_{equil}$ at 279.15 K, to determine if increasing the annealing pressure decreased the hydrate number (method III). To address whether the measured hydrate compositions reflected the annealing conditions or the synthesis conditions, two samples were synthesized at 283.5 K and 9.9 MPa, or about one-third the synthesis pressure used for the other samples. One sample (011604B) was dissociated by heating to 287.15 K at 9.68 MPa (method IV). The other sample (011604A) was cooled to 180 K and 0.1 MPa, following a low-pressure pathway within the hydrate stability field, then dissociated by heating the sample to 282 K at 0.1 MPa (method V).

## Data Analysis

The amount of methane gas released by dissociation is measured using our flowmeter. The data analysis routine that converts the load-cell output into a measurement of the moles of gas has been described previously.[13] With the propagation of measurement errors, the accuracy of the measured gas yield is $\pm$1 mol % for dissociation of a 30-g methane hydrate sample at 0.1 MPa. However, additional corrections must be made to obtain the gas yields in the elevated pressure experiments. The effects of increasing temperature and increasing volume on the amount of free gas in the pressure vessel, the amount of dissolved methane in the water produced by dissociation, and the contribution of the partial pressure of water to the total pressure must be taken into account before an accurate final gas yield can be determined.

The amount of free methane gas ($n_{g,free}$) in the pressure vessel can be calculated from the *P*, *V*, and *T* of the system using

$$n_{g,free} = \frac{PV}{ZRT} \tag{5}$$

where *R* is the gas constant 8.314 J/(mol K) and *Z* is the compression factor. The compression factor was obtained using

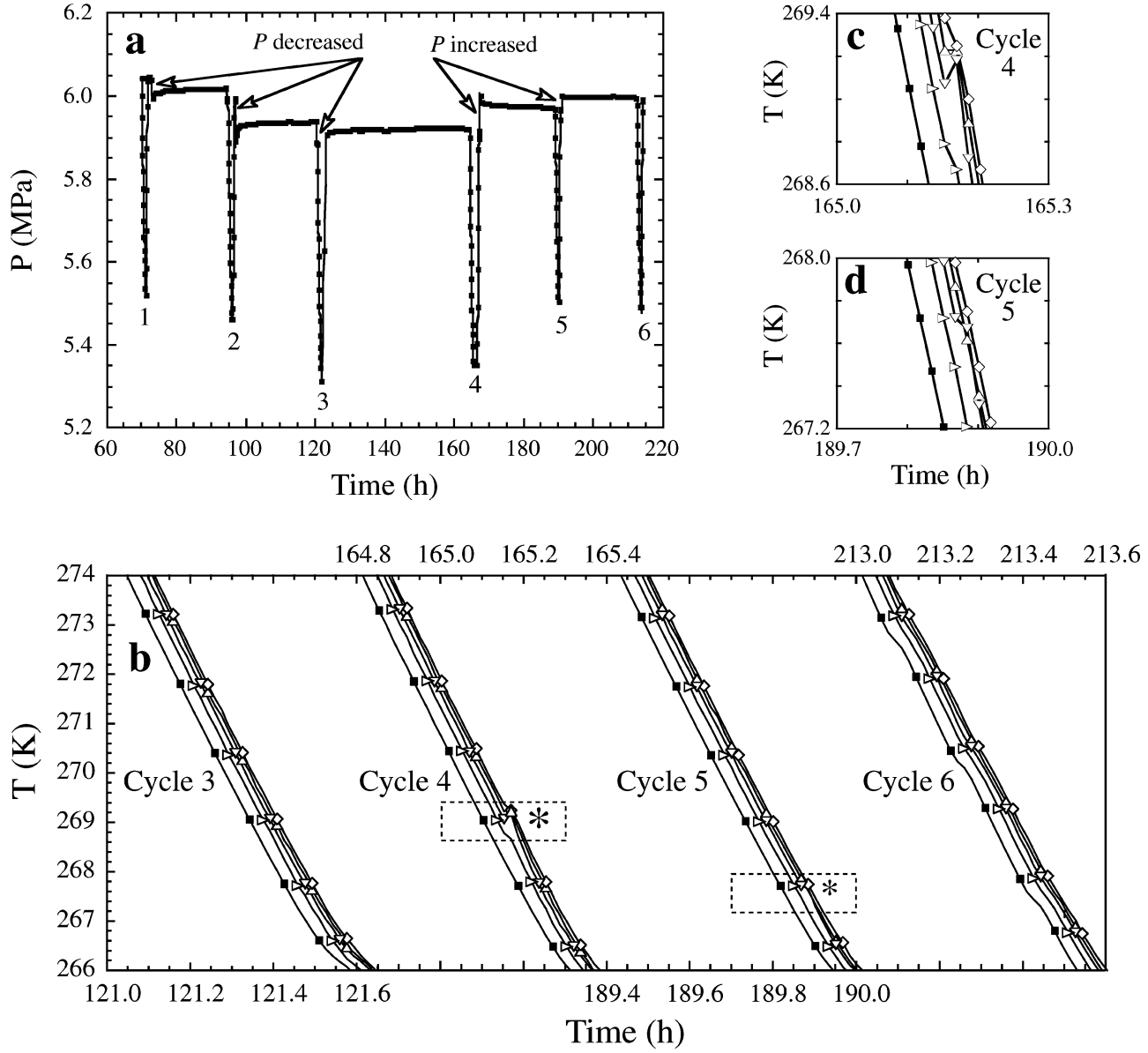


**Figure 2.** Example of method II for annealing samples at equilibrium conditions. In this experiment (100903B), the methane hydrate sample was first annealed at 281.15 K and 6.05 ± 0.02 MPa for 70 h, during which time some methane was released from the sample and collected by the flowmeter (not shown, see text). The sample was then isolated from the back-pressure regulator and flowmeter and thermally cycled six times from 281.15 K to a minimum of 260−265 K, following isothermal holds at various pressures. (a) The sample pressure history, showing that *P* was either manually decreased or increased before (cycle 3) or after (cycles 1, 2, 4, and 5) each thermal cycle. Note that the minimum *P* depended on the minimum *T* reached in a cycle. (b) The sample temperature history during cooling in cycles 3−6. External bath temperature (■) and sample temperatures (top △, middle ◇, bottom ▽, side right triangle) are shown. No ice point signal was detected during the cooling stage of cycles 1−3. A freezing anomaly (*) was observed during cycle 4, diminished in cycle 5, and had vanished in cycle 6. The freezing anomalies, occurring within the dotted boxes, are shown in greater detail in parts c and d. Note that, based on prior experience in detecting freezing anomalies following hydrate synthesis, the signal is stronger during cooling than heating and not detectable in the pressure record unless the thermal signal is greater than 1 K. Every fifth data point has been plotted in parts a and b; all points are plotted in parts c and d.

the equation of state for methane of Sychev et al.[17] The amount of free gas in the pressure vessel was calculated at the *P*, *V*, and *T* conditions both before and after dissociation (Table 2). When initial conditions were at pressures below the quadruple point, the final conditions were established after all ice product had melted. Values for $T_{initial}$, $T_{final}$, and $P_{initial}$ were determined by direct measurement. $P_{final}$ was corrected for the partial pressure of $H_2O$ using the Claussius−Clapeyron equation

$$P = P^* \exp\left\{\frac{\Delta H_{vap}}{R}\left(\frac{1}{T} - \frac{1}{T^*}\right)\right\} \qquad (6)$$

where $P^*$,$T^*$ is defined as the $H_2O$ triple point at $6.105 \times 10^{-4}$ MPa and 273.16 K and the enthalpy of vaporization, $\Delta H_{vap}$, is 45 050 J/mol.

The free gas volume in the pressure vessel was equal to the vessel volume less the volume of various metal spacers and the volume of methane hydrate or $H_2O$(l) in the vessel. The volume of the liquid water product ($V_w$) was calculated based on the mass of seed ice used to make the hydrate sample and the molar volume of water[18] at $T_{final}$ (assuming that the effect of pressure on $V_w$ is negligible). The methane hydrate unit cell volume was extrapolated from diffraction data collected between 4 and 170 K at 0.1 MPa.[19] Because the methane hydrate started to break down above 170 K, an extrapolation of up to 115 K is required to predict the molar volumes at the temperatures of

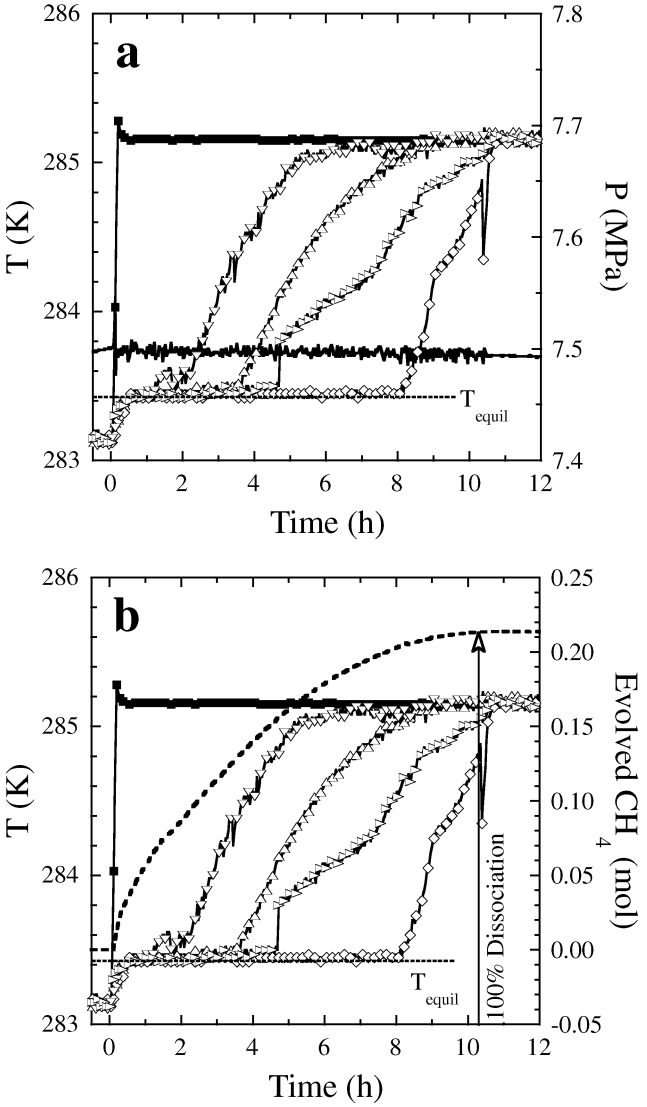


**Figure 3.** Example of methane hydrate dissociation via reaction 2. In this experiment (090903B), the methane hydrate sample was annealed at 283.15 K and 7.50 MPa (Table 1) before heating the surrounding bath to 285.15 K. (a) *P*,*T* history during dissociation. Bath temperature (■) and internal sample temperatures (top △, middle ◇, bottom ▽, side right triangle) are shown. The back-pressure regulator maintained a constant pressure (−) to within ±0.02 MPa during dissociation. While the bath *T* rose quickly to 285.15 K, the temperature in the sample stalled at equilibrium conditions while dissociation proceeded at the thermocouple location, before climbing to the bath *T*. (b) Gas evolution due to hydrate dissociation (···), with bath and sample *T* plotted again for reference. The amount of gas shown does not include corrections applied during data analysis (see text). Every fifth data point has been plotted.

interest. Extrapolations were based on second- and third-order polynomial fits to the data as well as a linear extrapolation of the data between 85 and 170 K. The uncertainty in the estimated hydrate volume is about ±0.8% at 273 K. Below, we report the results for the second-order fit and assess the uncertainties in hydrate number that arise when a slightly higher (third-order) or lower (first-order) estimate of the methane hydrate molar volume at $T_{initial}$ is used. The molar hydrate volume was calculated on the basis of $cm^3$/mol $H_2O$ from the equation

$$V_{hyd}(cm^3/\text{mol } H_2O) = \frac{V_{hyd}(Å^3)}{46H_2O}\frac{cm^3}{10^{24}Å^3}\frac{6.022 \times 10^{23}}{\text{mol}} \quad (7)$$

The volume of hydrate in the vessel (in $cm^3$) is obtained by multiplying by the number of moles of $H_2O$, namely, the starting mass of seed ice ($g_{ice}$, Table 2) divided by the molecular weight (in g/mol). In going from the initial to final conditions, *T* increases, *P* is approximately constant, and the free volume increases significantly. The net effect on the amount of free gas in the vessel is that it increases, namely, because $\Delta V$ of the nongaseous phases, $V_w - V_{hyd}$, is large and negative. In other words, some of the gas evolved from hydrate dissociation occupies this additional free volume and is not released to the flowmeter. This important correction ($\Delta n_{g,free}$) is listed in Table 3.

**TABLE 2: Initial and Final *P*,*T*,*V* Conditions for Methane Hydrate Dissociation Experiments and the Amount of Ice Used to Make the Methane Hydrate Sample**

| experiment ID | $T_{initial}$ (K) | $P_{initial}$ (MPa) | $V_{initial}$[a] ($cm^3$) | $T_{final}$ (K) | $P_{final,corr}$ (MPa) | $V_{final}$ ($cm^3$) | $g_{ice}$ (g) |
|---|---|---|---|---|---|---|---|
| 050203B | 263.09 | 1.88 | 28.43[b] | 275.05 | 1.85 | 34.97 | 26.03 |
| 051304A | 268.15 | 2.27 | 26.92 | 275.16 | 2.21 | 33.34 | 26.03 |
| 082003B | 273.15 | 2.74 | 18.10 | 275.12 | 2.74 | 24.56 | 26.05 |
| 100903A | 275.15 | 3.47 | 26.84 | 277.15 | 3.48 | 33.32 | 26.05 |
| 051304B | 275.15 | 3.28 | 25.57 | 277.14 | 3.28 | 32.05 | 26.03 |
| 110403B | 277.15 | 4.05 | 23.52 | 279.15 | 4.05 | 30.00 | 26.01 |
| 120303B | 279.15 | 4.81 | 23.50 | 281.15 | 4.81 | 30.00 | 26.01 |
| 120303A | 279.15 | 9.61 | 20.13 | 287.64 | 9.61 | 26.62 | 26.00 |
| 100903B | 281.15 | 6.00 | 23.47 | 283.15 | 6.00 | 29.99 | 26.02 |
| 090903B | 283.15 | 7.50 | 24.92 | 285.15 | 7.50 | 31.45 | 26.02 |
| 011604A | 184.44 | 0.10 | 22.06 | 282.06 | 0.100 | 27.90 | 26.06 |
| 011604B | 284.16 | 9.68 | 24.21 | 287.15 | 9.69 | 30.75 | 26.03 |
| 042204B | 285.15 | 9.07 | 25.53 | 287.14 | 9.07 | 32.06 | 26.00 |
| 090903A | 285.15 | 9.63 | 25.35 | 287.14 | 9.63 | 31.88 | 26.00 |

[a] $V_{initial}$ calculated using the second-order polynomial fit to unit cell data (see text). [b] $V_{initial}$ for this experiment was calculated by measuring the amount of gas released to the flowmeter when *P* was decreased from 2.02 to 1.86 MPa at 263.09 K.

Last, some methane remains dissolved in the water product. The amount of dissolved methane ($n_{g,diss}$) at $P_{final}$,$T_{final}$ was calculated using the Henry's Law constants in Sloan.[1] The net yield of methane gas, following dissociation of the hydrate sample, is then

$$n_{g,hyd} = n_{g,meas} + \Delta n_{g,free} + n_{g,diss} \quad (8)$$

where $n_{g,meas}$ is the gas measured by the flowmeter. To ascertain the reliability of the corrected gas yields, we compared the sum of $n_{g,hyd}$ and the gas released during the initial anneal ($n_{g,ann}$, before thermal cycling in method II) to the expected gas yield for $n_w = 5.89$, based on previous measurement of the composition of the "as-synthesized" methane hydrate. The uncertainty in the flowmeter measurement is ±1 mol % of the gas yield. Because samples are depressurized to the annealing conditions and then gas collection is immediately begun, excess methane gas may be adsorbed on the methane hydrate surface and released over time, which will increase $n_{g,ann}$ and result in high yields. There is some uncertainty in the large correction to $\Delta n_{g,free}$ as well as $V_{hyd}$. All measured gas contents are within ±4% of the expected yields (Table 3). Thus, the agreement between expected and measured gas yields is acceptable. Within the generously assessed uncertainty of ±4%, the measured hydrate numbers have an uncertainty of ±0.2.

## Results and Discussion

The measured hydrate numbers are shown next to the final *P*,*T* conditions prior to dissociation for each sample (Figure 4). We also show the results of two anneals of methane hydrate,

**TABLE 3: Measured and Corrected Gas Yields, Calculated Hydrate Numbers, and Comparison of Expected to Measured Gas Yields**

| experiment ID | $n_{g,meas}$ (mol) | $\Delta n_{g,free}$ (mol) | $n_{g,diss}$ (mol) | $n_{g,hyd}$ (mol) | $n_w$ | range for $n_w$[a] | $n_{g,ann}$ (mol) | $n_{g,exp}$ (mol) | $\Delta$ (%)[b] |
|---|---|---|---|---|---|---|---|---|---|
| 050203B | 0.2320 | 0.0038 | 0.0012 | 0.2370 | 6.10 | | 0.0021 | 0.2453 | −2.5 |
| 051304A | 0.2383 | 0.0048 | 0.0014 | 0.2445 | 5.91 | 5.90−5.92 | 0.0060 | 0.2453 | 2.1 |
| 082003B | 0.2297 | 0.0081 | 0.0017 | 0.2395 | 6.04 | 6.03−6.05 | 0.0041 | 0.2455 | −0.7 |
| 100903A | 0.2306 | 0.0103 | 0.0020 | 0.2429 | 5.95 | 5.94−5.97 | 0.0060 | 0.2455 | 1.4 |
| 051304B | 0.2295 | 0.0097 | 0.0019 | 0.2411 | 5.99 | 5.98−6.01 | 0.0062 | 0.2453 | 0.8 |
| 110403B | 0.2253 | 0.0120 | 0.0022 | 0.2396 | 6.03 | 6.02−6.04 | 0.0075 | 0.2451 | 0.8 |
| 120303B | 0.2213 | 0.0143 | 0.0025 | 0.2381 | 6.06 | 6.05−6.09 | 0.0064 | 0.2451 | −0.3 |
| 120303A | 0.2186 | 0.0255 | 0.0043 | 0.2484 | 5.81 | 5.78−5.85 | 0.0033 | 0.2450 | 2.7 |
| 100903B | 0.2196 | 0.0181 | 0.0030 | 0.2407 | 6.00 | 5.98−6.03 | 0.0086 | 0.2452 | 1.7 |
| 090903B | 0.2137 | 0.0230 | 0.0035 | 0.2402 | 6.01 | 5.99−6.05 | 0.0056 | 0.2452 | 0.3 |
| 011604A | 0.2460 | −0.0003 | 0.0001 | 0.2457 | 5.89 | | | 0.2456 | |
| 011604B | 0.2073 | 0.0297 | 0.0044 | 0.2413 | 5.99 | 5.96−6.04 | | 0.2453 | |
| 042204B | 0.2152 | 0.0281 | 0.0041 | 0.2473 | 5.83 | 5.81−5.88 | 0.0057 | 0.2450 | 3.3 |
| 090903A | 0.2056 | 0.0300 | 0.0043 | 0.2400 | 6.01 | 5.98−6.06 | 0.0028 | 0.2450 | −0.9 |

[a] Range reflects the uncertainty related to $V_{hyd}$. The lower value uses the hydrate volume extrapolated from the third-order polynomial fit to the unit cell data, while the higher values used the linear extrapolation (see text). [b] $\Delta$ (%) = $(n_{g,hyd} + n_{g,ann} - n_{g,exp}) \times 100/n_{g,exp}$ and was calculated using the second-order polynomial fit to the unit cell data. $\Delta$ is ±2% for the linear fit, and ±4% for the third-order polynomial fit.

**TABLE 4: Parameters Used in Calculation of $n_w$ Using Thermodynamic Analysis of Reactions 1 and 2**

| | reaction 1 | | | reaction 2 | | |
|---|---|---|---|---|---|---|
| parameter[a] | ±14 K[b] | ±10 K | ±5 K | ±14 K | ±10 K | ±5 K |
| $b$ | 9.6616 | 10.254 | 11.102 | 31.231 | 30.280 | 29.115 |
| $m$ | −2379.4 | −2538.8 | −2768.9 | −8278.5 | −8015.4 | −7694.8 |
| $r^2$ | 0.993 | 0.997 | 0.992 | 0.996 | 0.991 | 0.942 |
| d$P$/d$T$ | 0.0819 | 0.0881 | 0.0965 | 0.2705 | 0.2655 | 0.2574 |
| $\Delta H$ | 17843 | 19251 | 21137 | 58090 | 57267 | 55711 |
| $n_w$ | 6.73 | 6.34 | 5.76 | | | |

[a] Parameters $b$ and $m$ are obtained from the fit to the phase equilibria data using eq 9, and $r^2$ is the correlation coefficient of the fit. The slopes of the phase equilibria curves at the quadruple point (d$P$/d$T$) are then calculated (see text). The following values were used for the molar volumes of the phases in eqs 10 and 11 (in cm$^3$/mol, at 272.85 K and 0.1 MPa): $V(CH_4) = 818.96$,[17] $V(H_2O,s) = 19.65$,[20] $V(H_2O,l) = 18.02$,[18] $V$(hyd) = 22.49[19] (second-order polynomial fit, see text). The molar volumes of the liquid and solid phases assume that the pressure effect is negligible. Note that changing $V$(hyd) based on the fit to the diffraction data results in changes in $n_w$ of ±0.01. Handa[8] obtained the following values: $\Delta H_1 = 18130 \pm 270$ J/mol, $\Delta H_2 = 54190 \pm 280$ J/mol (at 273.15 K and 0.1 MPa), and $n_w = 6.00 \pm 0.01$ (synthesis conditions at 253 K and 3.4 MPa). [b] Data ranges are based on a temperature range about the quadruple point.

in which samples were annealed near 250−252 K and 2.0 MPa for 12 days and 274 K and 4.5 MPa for 5.8 days. These anneals were conducted before the back-pressure regulator was used and hence were not performed under isobaric conditions in that the sample pressure increased as gas was released from the hydrate. Samples were then dissociated using method V, as described in the Experimental Methods section.

Several immediate points are clear from Figure 4. First, along the equilibrium curve, the hydrate number is constant at 5.99 ± 0.07. No systematic change in $n_w$ with increasing $P$ and $T$ is discernible. This applies to samples annealed both above and below the quadruple point. Second, if $P,T$ conditions move well above from the equilibrium boundary, then the hydrate number shows a systematic decrease (i.e., the gas content of the sample increases), but still lies within the uncertainty of the measurements. This is best illustrated by the two experiments at 279.15 K (120303B vs 120303A). Doubling the annealing pressure decreased the hydrate number from 6.1 to 5.8, which is approaching the "ideal" composition of 5.75, where all cages are filled with methane. Third, the annealing process on hydrate samples grown at high $P,T$ conditions yields near-equilibrium compositions representative of the annealing conditions. We have two lines of evidence supporting that the annealing process is achieving this goal. First, the samples synthesized at lower $P,T$ conditions (283.5 K and 9.9 MPa instead of the usual conditions of 290 K and 27 ± 3 MPa) yield values of $n_w$ between 5.89 and 5.99, within the composition range between the high $P,T$ synthesized material and the annealed material at the equilibrium boundary. These samples were never exposed to high methane pressures, yet the hydrate numbers are low. The slightly higher $CH_4$ content measured for sample 011604A may in part be due to physical adsorption of free methane gas on the hydrate surface at low temperature (180 K). It is not likely the source of the compositional differences observed at the warm temperatures used in the other experiments. Second, the two samples at 285.15 K bracket the hydrate number between 5.8 and 6.0. The lower hydrate number was obtained on a sample annealed with method I, while the higher hydrate number was obtained on a sample annealed with method II. In the latter case, the sample was partially dissociated and then reformed, with a small residual ice peak still discernible in the thermal cycling data (Table 1). The differences in measured $n_w$ are consistent with the annealing histories of these samples.

Our compositions are consistent with other direct measurements of the methane hydrate number published previously. The hydrate literature contains a wide range of values for $n_w$; however, we deem the results obtained by Handa[8] and by Galloway et al.[6] to be particularly reliable. In both studies, the data analysis of the gas yield was carefully executed. Complete conversion of $H_2O$ to hydrate was confirmed by calorimetry in Handa's experiments. In the Galloway et al. study, mechanical grinding during synthesis was used to promote complete reaction to hydrate, and their independent measurements of $n_w$, based on gas uptake during synthesis and gas release during dissociation, are in close agreement.

The directly measured methane hydrate compositions, however, are in conflict with the high $n_w$ values obtained from thermodynamic analysis of the Clapeyron slopes of the equi-

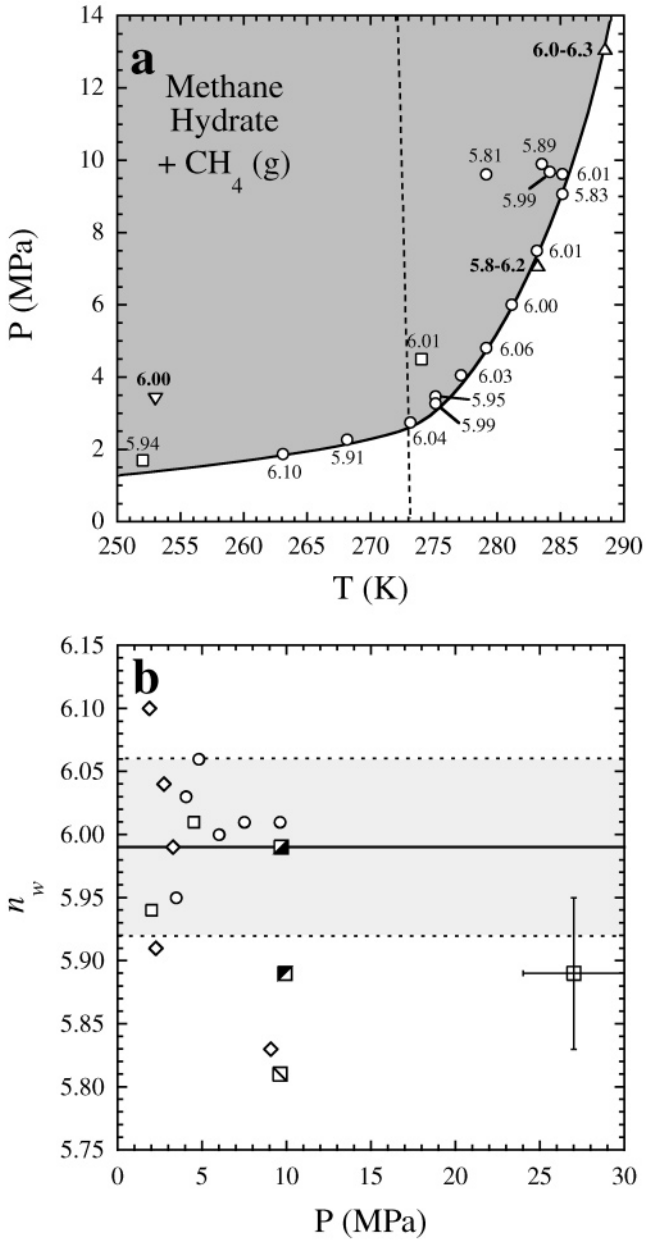


**Figure 4.** (a) Measured values for $n_w$ of methane hydrate at various $P,T$ conditions (○). The methane hydrate equilibrium boundary (−) is based on published phase equilibria data shown in Figure 1, and the solid/liquid boundary for $H_2O$ (- - -) is indicated. The results for two samples annealed under nonisobaric conditions (□, final $P,T$ conditions plotted, see text) and the results reported by Galloway et al.[6] (△) and Handa[8] (▽) ($n_w$ in bold) are also shown. (b) Hydrate compositions determined in this study (Table 3) at the final annealing pressures (Table 1). Samples were annealed at conditions just within the equilibrium boundary (◇, method I), reversed on the equilibrium boundary (○, method II), or annealed at elevated pressures well above the equilibrium boundary (⧅, method III). The conditions for the as-synthesized material are also shown (⊞, $P$ range and accuracy of composition indicated by error bars). Additionally, samples were synthesized at lower pressures near the equilibrium boundary then annealed further at slightly lower pressure (◪, method IV) before dissociation or cooled to low $T$ and dissociated at 0.1 MPa (◩, method V). Compositions of samples annealed under nonisobaric conditions are also plotted (□). The average value (−) with one standard deviation (shaded area) for all compositions of samples annealed on the equilibrium curve (methods I and II) are shown.

librium boundaries at the quadruple point. We repeated this type of analysis and discovered the source of variation for $n_w$. In our analysis, we fit the equilibrium data summarized in Sloan[1] for reactions 1 and 2 to equations of the form

$$\ln P = b + mT^{-1} \tag{9}$$

This form has been used previously to obtain the slopes of the reactions at the quadruple point and yields a linear relationship when fitting data covering a wide range of $P$ and $T$. Differentiating eq 9 after rewriting it in terms of $P$, we obtain the slope $dP/dT$ at the quadruple point. Rearranging eq 3, we obtain

$$\Delta H_1 = dP/dT^* \, T_Q^*(V_g + n_w V_{ice} - n_w V_{hyd}) \tag{10}$$

and

$$\Delta H_2 = dP/dT^* \, T_Q^*(V_g + n_w V_w - n_w V_{hyd}) \tag{11}$$

Note that $T_Q$ is the temperature at the quadruple point (272.85 K and 2.55 MPa,[16] which is corrected for the solution of methane in water). The hydrate molar volume is in units of $cm^3$/mol $H_2O$ (eq 7); hence it is multiplied by the number of moles of water. Equations 10 and 11 can be inserted into eq 4 and then solved for $n_w$. We calculated a value of 5997.9 J/mol for $\Delta H_{m,H_2O}$ at the quadruple point temperature using Kirchhoff's Law. The parameters obtained from eq 9, $\Delta H_1$, $\Delta H_2$, and $n_w$, are shown in Table 4. A wide range of values for the enthalpies of reaction and for $n_w$ are obtained, primarily based on the range of data that was fit. The calculations are highly sensitive to changes in the Clapeyron slopes, even when they vary by only a few percent. This, along with the assumption that the molar volume change of nongaseous phases is negligible, is the likely source of the high values above 7.0 cited for the $n_w$ of methane hydrate in earlier studies.[2,3] Clearly, direct measurement of the enthalpies of reactions 1 and 2 by calorimetry and of the gas content of the hydrate through dissociation yield the most reliable and consistent values.

As discussed above, there may be a small, systematic increase in methane hydrate gas content as $P,T$ conditions move away from the equilibrium boundary. In performing these measurements, we also expected to observe a decrease in $n_w$ with increasing pressure along the equilibrium boundary. This trend has been predicted by statistical thermodynamic models of hydrate equilibria[6,21] and demonstrated for other hydrates by direct measurement of hydrate composition.[7] However, in the case of the other hydrates, the compositional changes were observed at 273 K and over a very modest pressure range up to 0.5 MPa, above which the variation in $n_w$ with $P$ is becoming negligible. Methane hydrate is not even stable at these pressures, requiring a 5-fold increase in $P$ to reach the equilibrium boundary at 273 K. It is quite possible that at similarly low pressures (and very low temperatures) methane hydrate may exhibit comparable changes in $n_w$ with $P$, but at the higher pressures in this study the variation has become negligible. Of course, this does not explain the discrepancy between observed values and those predicted by statistical thermodynamics, a discussion that is beyond the scope of this paper. However, a hydrate number of 6.85 at the quadruple point,[21] calculated using this theory, is not supported by any direct measurement of methane hydrate composition to date.

Instead, experimental measurement of methane hydrate compositions indicate that there is little compositional variation at $P,T$ conditions of geological interest, namely, at conditions along the equilibrium boundary for reaction 2. A composition of approximately $CH_4 \cdot 5.8-6.0H_2O$ is expected, with $n_w$ decreasing slightly away from the hydrate equilibrium boundary. This simple result is encouraging for interpreting in situ methane

hydrate compositions and for assessing extents of decomposition in recovered samples of natural material. Our experimental measurements have been made on methane hydrate equilibrated in the presence of methane gas, leaving an open question as to whether methane hydrate in equilibrium with water also shows no compositional variation along the equilibrium boundary. The Raman spectroscopy experiments of Huo et al.[10] suggest that this hydrate is relatively methane-poor. If indeed that is the case, then one might expect that methane hydrate in equilibrium with water has a systematic offset to slightly higher values of $n_w$ but not much variability with pressure. Further experiments, utilizing both Raman spectroscopy and an independent means of determining total hydrate gas content, would be required to address this issue.

**Acknowledgment.** We thank I-Ming Chou, William F. Waite, and two anonymous reviewers for providing helpful comments during preparation of the manuscript. We acknowledge the support of the Gas Hydrate Project of the USGS, led by Debbie Hutchinson.

## References and Notes

(1) Sloan, E. D. *Clathrate Hydrates of Natural Gases*, 2nd ed; Marcel Dekker: New York, 1998.

(2) Roberts, O. L.; Brownscombe, E. R.; Howe, L. S.; Ramser, H. *Petrol. Eng.* **1941**, *12*, 56.

(3) Frost, E. M.; Deaton, W. M. *Oil Gas J.* **1946**, *45*, 170.

(4) Glew, D. N. *J. Phys. Chem.* **1962**, *66*, 605.

(5) de Roo, J. L.; Peters, C. J.; Lichtenthaler, R. N.; Diepen, G. A. M. *AIChE J.* **1983**, *29*, 651.

(6) Galloway, T. J.; Ruska, W.; Chappelear, P. S.; Kobayashi, R. *Ind. Eng. Chem. Fundam.* **1970**, *9*, 237.

(7) Cady, G. H. *J. Phys. Chem.* **1983**, *87*, 4437.

(8) Handa, Y. P. *J. Chem. Thermodyn.* **1986**, *18*, 915.

(9) Handa, Y. P. *J. Chem. Thermodyn.* **1986**, *18*, 891.

(10) Huo, A.; Hester, K.; Sloan, E. D. *AIChE J.* **2003**, *49*, 1300.

(11) Stern, L. A.; Kirby, S. H.; Durham, W. B. *Science* **1996**, *273*, 1843.

(12) Stern, L. A.; Circone, S.; Kirby, S. H.; Durham, W. B. *J. Phys. Chem. B* **2001**, *105*, 1756.

(13) Circone, S.; Kirby, S. H.; Pinkston, J. C.; Stern, L. A. *Rev. Sci. Instrum.* **2001**, *72*, 2709.

(14) Circone, S.; Stern, L. A.; Kirby, S. H.; Pinkston, J. C.; Durham, W. B. In *Gas Hydrates: Challenges for the Future*; Holder, G., Bishnoi, P., Eds.; New York Academy of Sciences: New York, 2000; p 544.

(15) Circone, S.; Stern, L. A.; Kirby, S. H. *J. Phys. Chem. B* **2004**, *108*, 5747−5755.

(16) Circone, S.; Stern, L. A.; Kirby, S. H. *Energy Fuels*, submitted for publication.

(17) Sychev, V. V.; Vasserman, A. A.; Zagoruchenko, V. A.; Kozlov, A. D.; Spiridonov, G. A.; Tsymarny, V. A. *Thermodynamic Properties of Methane*; Hemisphere Publishing Corporation: Washington, 1987.

(18) Dorsey, N. E. *Properties of Ordinary Water Substance*; Reinhold Publishing Corporation: New York, 1940.

(19) Rawn, C. J.; Chakoumakos, B. C.; Rondinone, A. J.; Stern, L. A.; Circone, S.; Kirby, S. H.; Ishii, Y.; Jones, C. Y.; Toby, B. H.; Sassen, R. Neutron and X-ray powder diffraction characterization of a variety of structure I and structure II clathrate hydrates, manuscript in preparation.

(20) Ginnings, D. C.; Corruccini, R. J. *J. Res., Natl. Bur. Stand.* **1947**, *38*, 583.

(21) Saito, S.; Marshall, D. R.; Kobayashi, R. *AIChE J.* **1964**, *10*, 734.